

---

---

# PET Measurement of Cardiac and Nigrostriatal Denervation in Parkinsonian Syndromes

David M. Raffel<sup>1</sup>, Robert A. Koeppe<sup>1</sup>, Roderick Little<sup>2</sup>, Chia-Ning Wang<sup>2</sup>, Suyu Liu<sup>2</sup>, Larry Junck<sup>3</sup>, Mary Heumann<sup>3</sup>, and Sid Gilman<sup>3</sup>

<sup>1</sup>Division of Nuclear Medicine, Department of Radiology, University of Michigan, Ann Arbor, Michigan; <sup>2</sup>Department of Biostatistics, University of Michigan, Ann Arbor, Michigan; and <sup>3</sup>Department of Neurology, University of Michigan, Ann Arbor, Michigan

---

Scintigraphic imaging with <sup>123</sup>I-metaiodobenzylguanidine (<sup>123</sup>I-MIBG) has demonstrated extensive losses of cardiac sympathetic neurons in idiopathic Parkinson's disease (IPD). In contrast, normal cardiac innervation has been observed in <sup>123</sup>I-MIBG studies of multiple-system atrophy (MSA) and progressive supranuclear palsy (PSP). Consequently, it has been hypothesized that cardiac denervation can be used to differentiate IPD from MSA and PSP. We sought to test this hypothesis by mapping the distribution of cardiac sympathetic neurons in patients with IPD, MSA, and PSP by using PET and <sup>11</sup>C-*meta*-hydroxyephedrine (<sup>11</sup>C-HED). Also, the relationship between cardiac denervation and nigrostriatal denervation was investigated by measuring striatal presynaptic monoaminergic nerve density with PET and <sup>11</sup>C-dihydrotrabenazine (<sup>11</sup>C-DTBZ).

**Methods:** <sup>11</sup>C-HED and <sup>11</sup>C-DTBZ scans were obtained for patients with IPD (*n* = 9), MSA (*n* = 10), and PSP (*n* = 8) and for age-matched control subjects (*n* = 10). Global and regional measurements of <sup>11</sup>C-HED retention were obtained to assess the extent of cardiac sympathetic denervation. <sup>11</sup>C-DTBZ binding was measured in the caudate nucleus, anterior putamen, and posterior putamen. **Results:** As expected, extensive cardiac denervation was observed in several of the patients with IPD. However, substantial cardiac denervation was also seen in some patients with MSA and PSP. <sup>11</sup>C-DTBZ studies demonstrated striatal denervation in all patients with IPD and in most patients with MSA and PSP. No correlation was found between cardiac <sup>11</sup>C-HED retention and striatal <sup>11</sup>C-DTBZ binding.

**Conclusion:** Cardiac sympathetic denervation was found to occur not only in IPD but also in other movement disorders, such as MSA and PSP. This finding implies that scintigraphic detection of cardiac sympathetic denervation cannot be used independently to discriminate IPD from other movement disorders, such as MSA and PSP. Cardiac sympathetic denervation was not correlated with striatal denervation, suggesting that the pathophysiologic processes underlying cardiac denervation and striatal denervation occur independently in patients with parkinsonian syndromes. These findings provide novel information about central and peripheral denervation in patients with neurodegenerative disorders.

**Key Words:** Parkinson's disease; multiple-system atrophy; progressive supranuclear palsy; PET; *meta*-hydroxyephedrine; dihydrotrabenazine

**J Nucl Med 2006; 47:1769-1777**

---

**I**diopathic Parkinson's disease (IPD) is associated with several autonomic manifestations, including gastrointestinal and genitourinary dysfunction and orthostatic hypotension. Patients with IPD who have orthostatic hypotension show decreased levels of norepinephrine in plasma and supersensitivity to norepinephrine infusion, indicating postganglionic sympathetic denervation (1). Multiple studies of IPD with planar scintigraphy or SPECT with <sup>123</sup>I-metaiodobenzylguanidine (<sup>123</sup>I-MIBG), a false neurotransmitter taken up presynaptically by postganglionic sympathetic neurons innervating cardiac muscle, have shown striking reductions in myocardial <sup>123</sup>I-MIBG uptake, indicating cardiac sympathetic denervation (2-18). Cardiac sympathetic denervation has been found in patients with IPD but without orthostatic hypotension, although to a lesser degree than in those with orthostatic hypotension (17,19). Although some investigators found cardiac sympathetic denervation in the early stages of IPD (7,10,11,13), others reported it only in cases at later stages (3,8). The neuropathologic basis of the denervation appears to be neurodegenerative, with Lewy body deposition in the cardiac plexus (20).

Several investigations of IPD with <sup>123</sup>I-MIBG have included comparisons with 2 other parkinsonian syndromes, multiple-system atrophy (MSA) and progressive supranuclear palsy (PSP). Most have shown no abnormality in either MSA or PSP (6,8-10,12,13,15). Indeed, some investigators consider cardiac imaging with <sup>123</sup>I-MIBG to be a means of differentiating IPD from other parkinsonian syndromes and to be particularly helpful in separating patients with IPD and with prominent autonomic symptoms from those with MSA (6,9,10,13,15,21). Although these investigations suggested that cardiac imaging can differentiate IPD from MSA and PSP, a few studies reported reduced uptake in both of these disorders, although the reductions reported were smaller than those in IPD (2,4,22).

---

Received Jun. 16, 2006; revision accepted Aug. 21, 2006.

For correspondence or reprints contact: David M. Raffel, PhD, Division of Nuclear Medicine, Department of Radiology, University of Michigan Medical School, 3480 Kresge III Bldg., Ann Arbor, MI 48109-0552.

E-mail: raffel@umich.edu

PET offers higher sensitivity and more accurate measurements of tissue radioactivity concentrations than single-photon scintigraphy. PET with the sympathetic nerve tracer  $^{11}\text{C}$ -*meta*-hydroxyephedrine ( $^{11}\text{C}$ -HED) not only provides quantitative measurements of cardiac tracer retention, reflecting sympathetic nerve density, but also allows for the detailed assessment of regional variations in left ventricular innervation (23,24). In this study, we used PET with  $^{11}\text{C}$ -HED to investigate the hypothesis that cardiac denervation is exclusive to IPD and as such can be used as a clinical measure to differentiate IPD from other movement disorders, such as MSA and PSP. We also measured striatal presynaptic monoaminergic nerve density with  $^{11}\text{C}$ -dihydrotrabenazine ( $^{11}\text{C}$ -DTBZ), a radioligand for the vesicular monoamine transporter (VMAT2), to determine whether the central and peripheral nervous system degenerative processes occur in parallel. Previous studies with  $^{123}\text{I}$ -MIBG demonstrated that essentially all subjects with more advanced stages of IPD (Hoehn–Yahr stages 3–5) have severe cardiac denervation (3,8,22). Because of this finding, we chose to study subjects with relatively early stages of IPD (Hoehn–Yahr stages 1 and 2) with the goal of including subjects with a wider range of cardiac innervation levels than would be seen in more advanced IPD. A preliminary version of this work was presented elsewhere (25).

## MATERIALS AND METHODS

### Study Population

The Institutional Review Board of the University of Michigan approved this investigation. Informed consent was obtained from all participants. The subjects studied included 9 patients who had IPD and who were  $62 \pm 15$  y old (mean  $\pm$  SD; range, 35–77 y; 1 woman and 8 men), 10 patients who had MSA and who were  $62 \pm 7$  y old (range, 53–77 y; 3 women and 7 men), 8 patients who had PSP and who were  $71 \pm 6$  y old (range, 63–80 y; 6 women and 2 men), and 10 healthy control subjects who were  $61 \pm 9$  y old (range, 43–72 y; 6 women and 4 men). The diagnoses were based on published criteria for each of the disorders, IPD (26), MSA (27), and PSP (28).

Cardiac denervation occurs in diabetes mellitus (29–31); hence, subjects with this disorder were excluded. Because cardiac  $^{11}\text{C}$ -HED uptake can be influenced by cocaine (32) and tricyclic antidepressants such as desipramine (33), subjects known to be taking these drugs were excluded from the study. Several of the patients with neurodegenerative diseases were taking an antidepressant medication, including the selective serotonin reuptake inhibitors (SSRIs) fluoxetine, paroxetine, citalopram, and sertraline. Among the patients with IPD, 3 took an SSRI and 1 took trazodone. In the patients with MSA, an SSRI was taken by 6, trazodone was taken by 1, and bupropion was taken by 1. Among the patients with PSP, 2 were taking an SSRI and 3 were taking trazodone. Because the uptake of  $^{11}\text{C}$ -HED into cardiac sympathetic neurons is mediated exclusively by the norepinephrine transporter (NET) and because none of these antidepressants possesses a high affinity for NET (34), these medications are unlikely to influence cardiac  $^{11}\text{C}$ -HED uptake. All 9 patients with IPD were taking dopaminergic medications; 7 were taking

carbidopa/levodopa, and 2 were taking pramipexole. Three patients with MSA were taking carbidopa/levodopa, and 2 were taking pramipexole. Three patients with PSP were taking carbidopa/levodopa.

### Radiochemistry

$^{11}\text{C}$ -HED was prepared by  $^{11}\text{C}$  methylation of (–)-metaraminol as the free base and purified by high-performance liquid chromatography (35). This procedure provided  $^{11}\text{C}$ -HED at specific activities of 18.5–55.5 TBq/mmol and radiochemical purities of greater than 98%.  $^{11}\text{C}$ -DTBZ was prepared by  $^{11}\text{C}$  methylation of  $\alpha$ -(+)-9-*O*-desmethyldihydrotrabenazine with a solid-phase support system allowing purification and isolation of the product,  $^{11}\text{C}$ -DTBZ, without high-performance liquid chromatography purification (36). Specific activities were  $>59.2$  TBq/mmol, and radiochemical purities were greater than 95%.

### PET Imaging

With the patient lying comfortably in the PET scanner,  $740 \pm 74$  MBq (mean  $\pm$  SD) of  $^{11}\text{C}$ -HED was injected intravenously, and a dynamic sequence of scans of the heart was acquired for 40 min. At 2 h after the injection of  $^{11}\text{C}$ -HED,  $666 \pm 66$  MBq of  $^{11}\text{C}$ -DTBZ was injected intravenously, and a dynamic sequence of scans of the brain was acquired for 60 min. All scans were obtained with a Siemens ECAT EXACT-HR + PET scanner, which has an intrinsic resolution of  $\sim 4.6$  mm full width at half maximum (FWHM). Sixty-three planes with a 2.425-mm center-to-center separation were imaged simultaneously. Attenuation correction was performed by reconstruction of measured transmission scan data, which was then segmented and reprojected back into sinogram space. The resolution of the reconstructed images was approximately 8–9 mm at FWHM for the  $^{11}\text{C}$ -HED scans and 6.0–6.5 mm at FWHM for the  $^{11}\text{C}$ -DTBZ scans. For the  $^{11}\text{C}$ -DTBZ studies, pixel-by-pixel fits with a reference region Logan plot analysis were performed (37). This analysis provided parametric images of the total tissue distribution volume ratio (DVR) for  $^{11}\text{C}$ -DTBZ relative to a reference region (occipital cortex) and parametric images of ligand transfer from plasma to brain. For measurements in the caudate nucleus, anterior putamen, and posterior putamen, anatomically configured volumes of interest were created from parametric images of the DVR. For  $^{11}\text{C}$ -HED, images from the heart scan were resliced by a computer algorithm into short-axis images for further quantitative analysis as previously described (38). A region of interest was placed over the left ventricular chamber in a short-axis slice near the base of the heart, and a time–activity curve for total activity in blood versus time was generated. Next, the left ventricular wall in each of the 8 short-axis slices from the apex to the base was automatically subdivided into 60 angular sectors to generate a total of 480 sectors. The time–activity curve for tissue  $^{11}\text{C}$ -HED concentration versus time was determined for each sector. As a semiquantitative measure of nerve density and neuronal integrity, tissue  $^{11}\text{C}$ -HED concentrations in the final image frame (30–40 min after injection) were normalized by dividing by the integral of the blood time–activity curve over the 40-min scan. This procedure provided for each myocardial region an  $^{11}\text{C}$ -HED retention index (RI; mL of blood/min/mL of tissue), which reflects the ability of the sympathetic neurons to take up and store norepinephrine. RI values for the 10 healthy control subjects were used to define a normal control database, in which the mean and SD for each myocardial sector were calculated and stored in the conventional polar map format used in nuclear cardiology. Measured RI data for each patient with a neurodegenerative disorder

were compared with this healthy control database by use of  $z$  score analysis. For this analysis, a  $z$  score was calculated for each sector in a patient's polar map as follows:  $z_i = (\mu_i - q_i)/\sigma_i$ ; in this equation,  $q_i$  is the patient's RI value for the  $i^{\text{th}}$  sector of the polar map,  $\mu_i$  is the healthy population mean RI for that sector, and  $\sigma_i$  is the corresponding across-subject SD of the healthy population for that sector. Left ventricular sectors with  $z$  scores of more than 2.5 (i.e., their  $^{11}\text{C}$ -HED RI values were more than 2.5 SDs below the healthy population mean) were considered to have abnormal  $^{11}\text{C}$ -HED retention. The fraction of 480 sectors in each patient's polar map that were abnormal was calculated as a measure of the extent of abnormal  $^{11}\text{C}$ -HED retention in the left ventricle. In addition, regional extent measures were also generated for 3 large regions of the left ventricle on the basis of the left ventricular regions perfused by the 3 main coronary arteries: left circumflex artery (LCX), left anterior descending artery (LAD), and right coronary artery (RCA).

### Statistical Analysis

Analysis of variance was conducted to compare the mean levels of binding of  $^{11}\text{C}$ -DTBZ in the striatum between groups. For the mean RI values for  $^{11}\text{C}$ -HED in the heart, the use of analysis of variance was considered inappropriate because the distributions of values from patients were clearly nongaussian. Our interest lay in identifying patients with  $^{11}\text{C}$ -HED retention outside the normal range rather than the overall mean for each patient subgroup. To test for abnormal  $^{11}\text{C}$ -HED retention, a  $t$  statistic was computed for values from each patient by subtracting the control mean and dividing by the control SD. One-sided  $P$  values were then computed for whether an  $^{11}\text{C}$ -HED retention value as small as that observed could have arisen in the healthy population. These  $P$  values are presented without corrections for multiple comparisons but remained highly significant even after such corrections.

## RESULTS

### Patient Characteristics

The patients with IPD were generally in the early to middle phases of the disorder, with disease durations varying from 3 to 9 y and with Hoehn–Yahr scores of 1.5–2.5. Only 1 patient had symptoms of orthostatic hypotension; none had urinary retention or incontinence, and none had diabetes mellitus. The patients with MSA had various durations of symptoms (3–12 y) and had different degrees of ataxia and parkinsonism, but all had sufficient postural hypotension or urinary incontinence to qualify for the diagnosis of probable MSA. Two patients had severe intensity of both parkinsonian symptoms and postural hypotension, and a third patient had severe ataxia and postural hypotension but minimal parkinsonism. None of the patients with MSA had diabetes mellitus. The patients with PSP had various durations of symptoms (3–9 y) and various intensities of parkinsonism, but all had marked impairment of voluntary upgaze, downgaze, or both, absence of convergence, presence of square wave jerks, and positive responses to oculocephalic stimulation. One patient with PSP had a history of borderline diabetes mellitus that was managed without medication.

### Cardiac $^{11}\text{C}$ -HED Retention

In the 10 control subjects, the mean and across-subject SD of the  $^{11}\text{C}$ -HED RI values was  $0.073 \pm 0.009$  mL of blood per minute per milliliter of tissue. Table 1 summarizes the clinical features and  $^{11}\text{C}$ -HED retention measures for the patients with neurodegenerative disorders. To facilitate the comparison of cardiac denervation and striatal denervation,  $^{11}\text{C}$ -DTBZ binding potential data for the posterior putamen are also provided in Table 1. In Figure 1, the global mean  $^{11}\text{C}$ -HED RI values (i.e., average RI for the entire left ventricle) for each subject are plotted. Figure 2 shows representative cardiac PET images and corresponding  $^{11}\text{C}$ -HED retention polar maps.

Of the 9 patients with IPD, 4 had extensive myocardial denervation, with very low mean RI values (1-sided  $P$  values were 0.0002, 0.0002, 0.0003, and 0.0004) and more than 96% of the left ventricle having abnormally low  $^{11}\text{C}$ -HED retention values. The remaining 5 patients with IPD had  $^{11}\text{C}$ -HED retention values within the normal range.

Of the 10 patients with MSA, 2 had severe and extensive left ventricular denervation ( $P = 0.0004$  for both cases). Two other patients with MSA had marginal global  $^{11}\text{C}$ -HED retention deficits ( $P = 0.03$  and  $0.06$ ; these 2  $P$  values would not be statistically significant after allowing for multiple comparisons). However, these 2 patients with MSA each had large regions of the left ventricle with statistically significant  $^{11}\text{C}$ -HED retention deficits, primarily in the LCX and RCA territories (Table 1; Fig. 2). Both patients with MSA and with severe global myocardial denervation had marked postural hypotension, akinesia, and urinary incontinence. One of these patients died after this study, and autopsy examination verified the diagnosis of MSA, with prominent degeneration of the pons, inferior olive, and cerebellum and with glial cytoplasmic inclusions positive for  $\alpha$ -synuclein. Only 1 other patient with MSA had a similar severe level of postural hypotension, and this patient had principally ataxia, with few signs of parkinsonism. This patient and the remaining 5 patients with MSA had global  $^{11}\text{C}$ -HED RI values within the normal range.

Two of the 8 patients with PSP had extensive areas of severe denervation (global extent of abnormal values: 66% and 81%) leading to global mean RI values that were significantly lower than control values ( $P = 0.0017$  and  $0.0038$ ), but they were not as low as those seen in the IPD and MSA patients with severe denervation. The remaining 6 patients with PSP had normal cardiac  $^{11}\text{C}$ -HED retention values.

Cardiac retention of  $^{11}\text{C}$ -HED did not appear to be influenced by the medications taken by the patients. In the 11 patients taking an SSRI,  $^{11}\text{C}$ -HED uptake was severely and globally decreased in 4, regionally decreased in 3, and essentially normal in 4. Among the 5 patients taking trazodone, 1 had a severe global decrease in  $^{11}\text{C}$ -HED uptake, and 4 had normal uptake. The 1 patient taking bupropion had fairly normal  $^{11}\text{C}$ -HED uptake. Patients taking no antidepressant included 2 with severe global decreases in uptake

**TABLE 1**

Clinical Features, Cardiac <sup>11</sup>C-HED Retention Measures, and <sup>11</sup>C-DTBZ Binding to Posterior Putamen in Patients with Neurodegenerative Diseases

Group	Patient	Sex	Age (y)	Intensity of*			Mean ± SD <sup>11</sup> C-HED RI (mL of blood/min/mL of tissue)	Extent of <sup>11</sup> C-HED retention deficit (%) <sup>†</sup>				<sup>11</sup> C-DTBZ posterior putamen BP (unitless) <sup>‡</sup>
				Park	Atax	Auto		Entire LV	LCX	LAD	RCA	
IPD	1	M	69	++	-	-	0.025 ± 0.003	97	100	95	100	0.61
	2	M	46	+	-	-	0.086 ± 0.020	-	-	-	-	0.40
	3	M	77	+	-	-	0.022 ± 0.004	100	100	100	100	0.68
	4	M	73	+	-	-	0.078 ± 0.009	-	-	-	-	0.49
	5	M	35	+	-	-	0.071 ± 0.011	-	-	-	-	0.72
	6	M	75	++	-	-	0.026 ± 0.003	97	100	96	100	0.68
	7	F	65	+	-	-	0.075 ± 0.011	-	-	-	-	0.71
	8	M	47	++	-	+	0.076 ± 0.010	-	-	-	-	0.38
	9	M	72	++	-	-	0.023 ± 0.003	96	100	93	100	0.73
MSA	1	M	70	+++	-	+++	0.027 ± 0.004	92	100	87	100	0.72
	2	M	59	+++	++	+++	0.026 ± 0.004	97	100	95	100	0.49
	3	F	77	+++	+++	++	0.089 ± 0.014	-	-	-	-	1.70
	4	M	62	+	+++	++	0.073 ± 0.007	-	-	-	-	0.54
	5	M	60	+++	+++	+++	0.061 ± 0.008	2	8	-	-	0.52
	6	M	57	+	++	++	0.084 ± 0.009	-	-	-	-	2.47
	7	F	61	-	+++	+++	0.070 ± 0.008	-	-	-	-	0.79
	8	F	59	+++	+++	+++	0.057 ± 0.009	23	71	2	38	0.76
	9	M	63	++	+++	+++	0.077 ± 0.011	-	-	-	-	2.27
	10	M	53	+	+++	+++	0.053 ± 0.006	21	32	5	71	2.34
PSP	1	F	68	+++	-	-	0.088 ± 0.008	-	-	-	-	0.86
	2	F	78	+	-	-	0.078 ± 0.013	-	-	-	-	2.01
	3	M	63	++	-	-	0.036 ± 0.008	81	95	72	100	0.34
	4	F	71	++	-	-	0.041 ± 0.009	66	100	49	100	0.56
	5	F	67	++	-	-	0.077 ± 0.013	-	-	-	-	1.06
	6	F	80	++	-	-	0.082 ± 0.014	1	-	1	-	0.51
	7	F	72	++	-	-	0.077 ± 0.017	-	-	-	-	0.92
	8	M	69	+	-	++	0.073 ± 0.015	-	-	-	-	0.53

\*Park = intensity of parkinsonian symptoms of akinesia, rigidity, tremor at rest, and hypokinetic speech; Atax = intensity of ataxia of gait, limbs, and speech; Auto = intensity of orthostatic blood pressure and pulse changes and urinary incontinence. Rating scale: - = normal; + = mild; ++ = moderate; +++ = marked.

<sup>†</sup>For patients with no regions of abnormal <sup>11</sup>C-HED retention, extent measures of 0% are represented by dash. Entire LV = fractional area of entire left ventricle (LV) that is denervated. Fractional areas of denervation in 3 coronary arteries (LCX, LAD, and RCA) are also given.

<sup>‡</sup><sup>11</sup>C-DTBZ binding potential (BP) in posterior putamen was calculated from measured DVR as BP = DVR - 1; in healthy control subjects, mean ± SD was 2.52 ± 0.32.

and 8 with normal uptake. In the 13 patients taking carbidopa/levodopa, <sup>11</sup>C-HED uptake was severely and globally reduced in 6, regionally decreased in 1, and normal in 6. None of the 4 patients taking pramipexole had any <sup>11</sup>C-HED retention abnormalities.

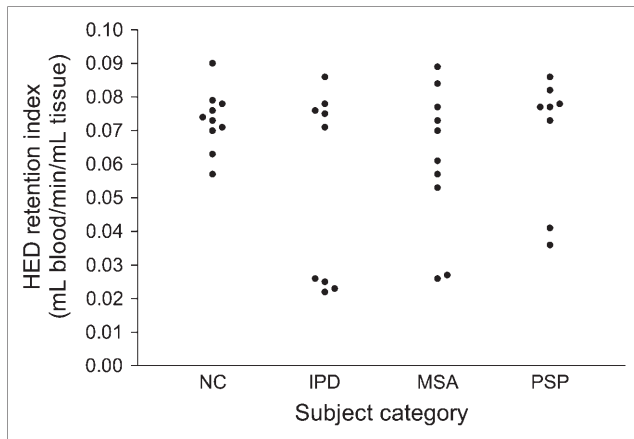
**Striatal <sup>11</sup>C-DTBZ Binding**

Table 2 shows <sup>11</sup>C-DTBZ binding potential data for the caudate nucleus, anterior putamen, and posterior putamen for the patients with IPD, MSA, and PSP in comparison with the healthy control subjects. All 3 groups of patients showed diminished binding compared with the healthy control subjects, and in the posterior putamen, the values for all 3 groups were more than 2 SDs below the values for the healthy control

subjects. All 3 groups of patients also showed a gradient, with lower binding values in the posterior putamen than in the caudate nucleus. These results persisted after adjustment for age by analysis of covariance.

**Relationship of Cardiac Retention to Putamen Binding**

There was no clear relationship between cardiac <sup>11</sup>C-HED retention and <sup>11</sup>C-DTBZ binding in the posterior putamen (Fig. 3). Similarly, no correlations were found between cardiac <sup>11</sup>C-HED retention and <sup>11</sup>C-DTBZ binding in the anterior putamen and the caudate nucleus or between cardiac <sup>11</sup>C-HED retention and the ratio of <sup>11</sup>C-DTBZ binding potentials in the caudate nucleus and the posterior putamen (data not shown). The 4 patients with IPD, the 2 patients with



**FIGURE 1.** Global mean  $^{11}\text{C}$ -HED RI values. NC = normal (healthy) control.

MSA, and the 2 patients with PSP who showed substantial decreases in global cardiac retention also showed markedly diminished posterior putamen binding potential; however, several IPD and MSA patients with normal levels of cardiac retention also showed markedly diminished posterior putamen binding potential. Two of the patients with MSA, both with the MSA-C type, showed essentially normal posterior putamen binding potential and normal levels of cardiac retention as well. Figure 4 shows parametric images of the  $^{11}\text{C}$ -DTBZ DVR at the level of the striatum and corresponding  $^{11}\text{C}$ -HED RI polar maps for representative subjects.

## DISCUSSION

MSA presents clinically with symptoms that are difficult to distinguish from those of IPD. Initial reports suggesting that cardiac denervation was exclusive to IPD were of great interest because it appeared that scintigraphic detection of cardiac denervation could be used as a single clinical measure capable of discriminating MSA from IPD. However, in the present study, contrary to many previous investigations (6,8–10,12,13,15), we found extensive denervation of cardiac postganglionic sympathetic fibers in 2 of 10 patients with probable MSA. One of these 2 patients died a few months after the present study, and the diagnosis of MSA was confirmed by neuropathologic examination of the brain. Two additional patients with MSA had substantial regional  $^{11}\text{C}$ -HED retention deficits. Sone et al. (39) recently reported neuropathologic changes in MSA that are likely to account for cardiac denervation. These investigators performed immunohistochemical examination of the sympathetic ganglia and brains of 26 patients with MSA and 19 age-matched control subjects. They found  $\alpha$ -synuclein-immunoreactive structures in the sympathetic ganglia of 42% of the patients with MSA and none in the control subjects. The immunoreactive structures proved to be Lewy bodies in several of the cases; in the others, they consisted of diffuse or focal neuronal cytoplasmic aggre-

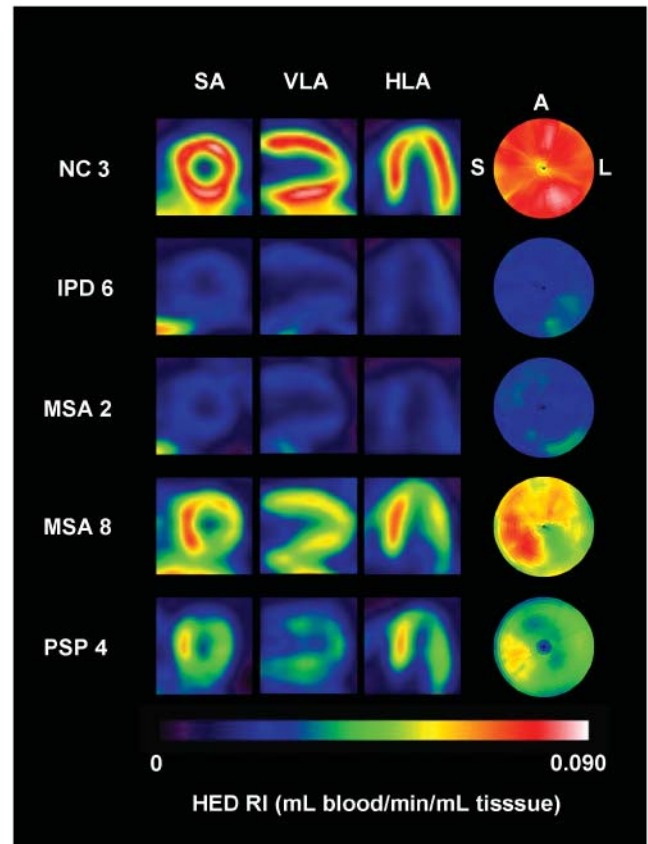


**FIGURE 2.** Representative parametric cardiac PET images and polar maps of  $^{11}\text{C}$ -HED retention. PET images are short-axis (SA), vertical long-axis (VLA), and horizontal long-axis (HLA) views for each subject. All PET images were normalized to integral of blood curve for each study, providing parametric  $^{11}\text{C}$ -HED RI images. PET images and polar maps of  $^{11}\text{C}$ -HED retention are all scaled to common maximum of 0.090 mL of blood per min per mL of tissue. For rainbow color table used, areas of low  $^{11}\text{C}$ -HED retention are shown in purple, blue and blue-green, moderate retention is shown in green and yellow, and normal retention is shown in orange, red, pink, and white. NC 3 images show high, uniform  $^{11}\text{C}$ -HED uptake in healthy control subject. IPD 6 images show extensive and severe denervation, as seen in 4 patients with IPD. MSA 2 images show extensive and severe denervation, as seen in 2 patients with MSA. MSA 8 images show nonuniform, more focal regional denervation, as seen in 2 patients with MSA. PSP 4 images show large regions of cardiac denervation, as seen in 2 patients with PSP. A = anterior wall; L = lateral wall; S = septal wall.

gates and swollen neurites, suggesting that these aggregates were progressing to become Lewy bodies. The mean disease duration for cases of MSA showing  $\alpha$ -synuclein-immunoreactive structures was significantly longer than that of cases of MSA not showing these structures. In the present study, our small sample limited our ability to infer the important variables that might lead to cardiac denervation in MSA. The patients with MSA and with extensive cardiac denervation (patients 1 and 2) had symptom durations of 10 and 3 y, respectively, but other patients without cardiac denervation had equal or longer durations of illness. These 2 severely affected patients had marked orthostatic

**TABLE 2**  
VMAT2 Transporter Densities in Brain

Group (n)	<sup>11</sup> C-DTBZ binding potential*			
	Caudate nucleus	Anterior putamen	Posterior putamen	AP gradient <sup>†</sup>
Control (10)	2.09 ± 0.25	2.48 ± 0.29	2.52 ± 0.32	0.83 ± 0.06
IPD (9)	1.30 ± 0.45 (63) [0.0010]	0.94 ± 0.32 (38) [4.3 × 10 <sup>-8</sup> ]	0.60 ± 0.14 (24) [1.8 × 10 <sup>-10</sup> ]	2.22 ± 0.69 [3.5 × 10 <sup>-9</sup> ]
MSA (10)	1.31 ± 0.75 (63) [0.0052]	1.30 ± 0.79 (53) [4.9 × 10 <sup>-4</sup> ]	1.26 ± 0.83 (50) [4.3 × 10 <sup>-4</sup> ]	1.13 ± 0.25 [0.0011]
PSP (8)	0.95 ± 0.38 (46) [5.8 × 10 <sup>-6</sup> ]	0.92 ± 0.48 (37) [2.9 × 10 <sup>-6</sup> ]	0.85 ± 0.53 (34) [3.9 × 10 <sup>-6</sup> ]	1.23 ± 0.35 [9.9 × 10 <sup>-4</sup> ]

\*For <sup>11</sup>C-DTBZ binding potentials, data shown are mean ± SD, percentage of normal mean in parentheses, and *P* value for single-tailed Student *t* test, assuming unequal variances between each patient group and healthy control group, in brackets.

<sup>†</sup>AP gradient = ratio of <sup>11</sup>C-DTBZ binding potentials in caudate nucleus and posterior putamen, calculated individually for each subject.

changes and moderate to severe urinary incontinence, suggesting extensive autonomic denervation, but 1 other patient (patient 7) had similarly severe orthostatic changes and urinary incontinence but no cardiac denervation. The 2 patients with MSA and with partial cardiac denervation had moderately severe orthostatic changes and severe urinary incontinence, suggesting that these patients may have later developed more extensive cardiac denervation.

In the present investigation, the cardiac <sup>11</sup>C-HED retention studies in patients with PSP also revealed findings contrary to those of several previous investigations, with severe denervation affecting large areas of the heart in 2 of the 8 patients. The 2 patients (patients 3 and 4) with cardiac denervation had disease durations of 5 and 9 y, respectively, but no urinary retention or incontinence and no orthostatic symptoms. The other patients with PSP had variable disease durations, some of 5–6 y but none as long as 9 y. One of the 2 patients with PSP and with cardiac denervation (patient 3) had diabetes mellitus, well controlled by diet alone. Although diabetes is associated with cardiac denervation, the pattern of myocardial sympathetic denervation

is entirely different from that seen in this patient. Diabetic involvement of sympathetic cardiac fibers affects the longest neurons initially; hence, denervation proceeds from the apex to the base, initially occurring only in the inferior and lateral walls. Ultimately, this process evolves to a consistent pattern of denervation in which only the neurons in the proximal segments of the septal and anterior walls are preserved (29–31). The striking difference between the regional pattern of cardiac denervation seen in our patient with PSP and the typical pattern seen in diabetics makes it unlikely that diabetes was the underlying cause of the observed myocardial denervation in our patient. One of the 2 patients with PSP who had cardiac denervation (patient 3) was being treated with carbidopa/levodopa, but 2 other patients without denervation (patients 5 and 6) received similar doses of carbidopa/levodopa. Review of the additional clinical findings in the 2 patients with partial denervation revealed no other features that separated them from the other patients with PSP who had normal retention values. The neuropathologic basis for the findings in these patients is not clear, as a literature search revealed no postmortem studies of sympathetic ganglia in PSP suggesting denervation of sympathetic ganglia. Only a single relevant study was found; it demonstrated a severely diminished sympathetic sweat response on the palm to deep breathing in PSP, suggesting an abnormality of sympathetic function in this disorder (40).

Previous studies of IPD with <sup>123</sup>I-MIBG documented that cardiac denervation generally occurs after the disease evolves beyond its earliest stages (Hoehn–Yahr stage 1), occurring in nearly all patients with more advanced stages of IPD (Hoehn–Yahr stages 3–5) (3,8,22). The 9 patients with IPD who were studied in the present work all were in the early to moderate stages of IPD (Hoehn–Yahr stages 1.5–2.5). Four of the 9 patients with IPD were found to have extensive cardiac denervation. Disease severity, as measured by Hoehn–Yahr stage, was not predictive of the presence or absence of extensive cardiac denervation. The 4 patients with IPD and with denervation had disease durations of 3–4 y. The 5 patients with <sup>11</sup>C-HED retention values in the normal range included 3 patients with disease durations as long as 7–9 y. Thus, within the small group of patients with IPD studied in the present work, there was no

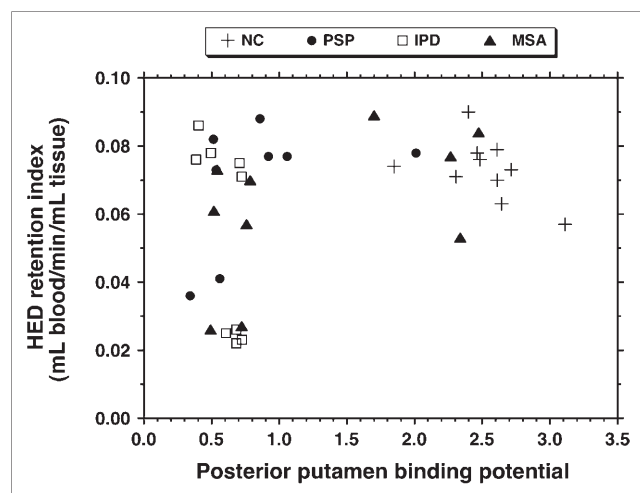


**FIGURE 3.** Relationship between cardiac innervation and striatal monoaminergic nerve density. Plotted is global mean <sup>11</sup>C-HED RI vs. <sup>11</sup>C-DTBZ binding potential in posterior putamen. NC = normal (healthy) control.

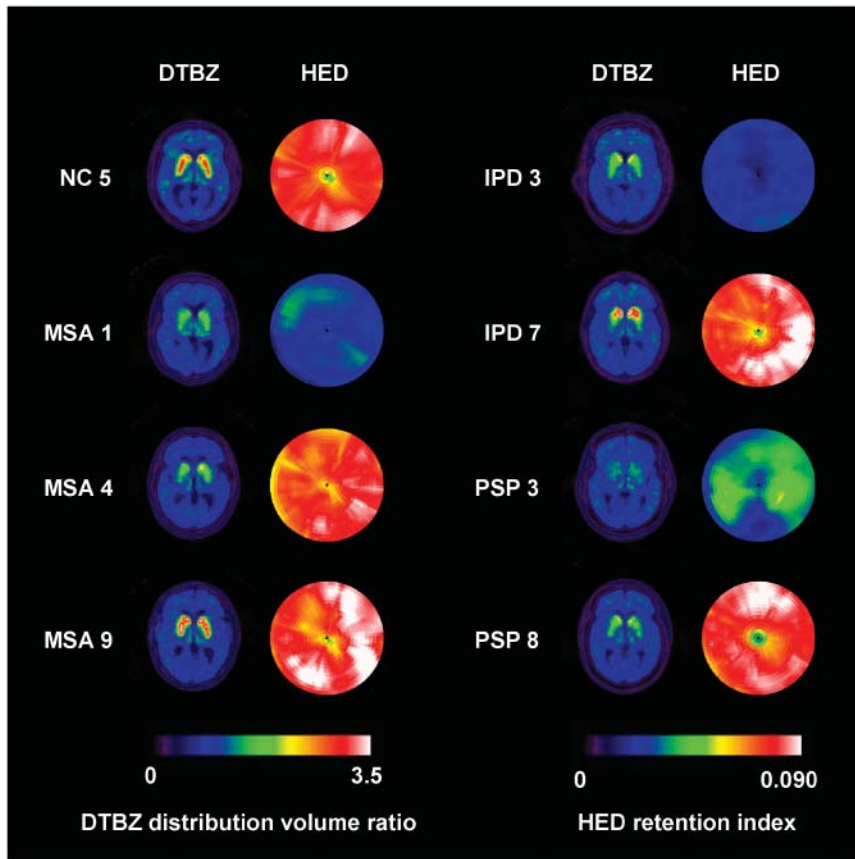


**FIGURE 4.** Representative parametric images of  $^{11}\text{C}$ -DTBZ DVR and corresponding  $^{11}\text{C}$ -HED RI polar maps. Parametric images of  $^{11}\text{C}$ -DTBZ DVR are all scaled to common maximum of 3.5. DVR is related to binding potential (BP) by equation  $\text{BP} = \text{DVR} - 1$  and is unitless. Polar maps of  $^{11}\text{C}$ -HED RI values are all scaled to common maximum of 0.090 mL of blood per min per mL of tissue. NC 5 images show high striatal binding of  $^{11}\text{C}$ -DTBZ and high, uniform cardiac retention of  $^{11}\text{C}$ -HED in healthy control subject. MSA 1 images show low striatal  $^{11}\text{C}$ -DTBZ binding and extensive severe cardiac denervation, as seen in 2 patients with MSA. MSA 4 images show low striatal  $^{11}\text{C}$ -DTBZ binding and normal uniform cardiac  $^{11}\text{C}$ -HED retention, as seen in 4 patients with MSA. MSA 9 images show normal striatal  $^{11}\text{C}$ -DTBZ binding and normal uniform cardiac  $^{11}\text{C}$ -HED retention, as seen in 4 patients with MSA. IPD 3 images show low striatal  $^{11}\text{C}$ -DTBZ binding and extensive severe cardiac denervation, as seen in 4 patients with IPD. IPD 7 images show low  $^{11}\text{C}$ -DTBZ binding in posterior putamen (with uncharacteristically well-preserved  $^{11}\text{C}$ -DTBZ binding in caudate nucleus) and normal uniform cardiac innervation, as seen in 5 patients with IPD. PSP 3 images show low striatal  $^{11}\text{C}$ -DTBZ binding and normal

nonuniform cardiac denervation, as seen in 2 patients with PSP. PSP 8 images show low striatal  $^{11}\text{C}$ -DTBZ binding and normal uniform cardiac denervation, as seen in 5 patients with PSP.

correlation between cardiac denervation and disease duration or disease severity.

Our  $^{11}\text{C}$ -HED results can be compared with those of a recent report by Nagayama et al. (22), who used  $^{123}\text{I}$ -MIBG to study the incidence of cardiac denervation in a large cohort of patients with parkinsonian syndromes. Included in their study were 45 patients with IPD at Hoehn–Yahr stages 1 and 2, 14 patients with MSA, and 7 patients with PSP. The fraction of each group found to have decreased cardiac  $^{123}\text{I}$ -MIBG retention at 4 h (expressed as a heart-to-mediastinum [H/M] ratio) was generally consistent with our observations for patients with IPD and MSA but different from those for patients with PSP. For IPD at Hoehn–Yahr stages 1 and 2, they found that 30 of 45 patients (67%) had decreased  $^{123}\text{I}$ -MIBG retention, and we found that 4 of 9 patients (44%) had extensive  $^{11}\text{C}$ -HED retention deficits. For MSA, they found that 3 of 14 patients (21%) had decreased  $^{123}\text{I}$ -MIBG retention, and we found that 2 of 10 patients (20%) had substantial  $^{11}\text{C}$ -HED retention deficits, with 2 more (20%) having focal regions of myocardial denervation. For PSP, they found that 6 of 7 patients (86%) had  $^{123}\text{I}$ -MIBG H/M ratios below normal, although the H/M ratios were higher than those seen in patients with IPD and with severe myocardial denervation. In contrast, we observed significant  $^{11}\text{C}$ -HED retention deficits in only 2 of 8 patients with PSP (25%). This discrepancy in the findings for PSP is compelling and suggests that further

studies with larger numbers of patients with PSP are needed to better characterize the impact of PSP on cardiac innervation. Apart from this discrepancy, there is considerable agreement between our 2 datasets.

The neuropathologic basis of cardiac denervation in IPD is neural degeneration with Lewy body deposition in the cardiac sympathetic plexus (20). Orimo et al. (41) used tyrosine hydroxylase (TH) immunohistochemistry to examine heart tissues from 5 control subjects, 11 patients with IPD, 8 patients with MSA, 5 patients with PSP, and several patients with dementia with Lewy bodies and Alzheimer's disease. They used the same methods to study sympathetic ganglia from control subjects and 5 patients with IPD. They found an almost total absence of TH-immunoreactive fibers in the heart tissues of most of the patients with IPD but preserved fibers in patients with PSP and all but 1 patient with MSA. TH immunoreactivity was preserved in the sympathetic ganglia of all but 1 patient with IPD. They concluded that cardiac postganglionic sympathetic denervation affects nerve fibers innervating the heart in advance of neuronal loss in the sympathetic ganglia. These findings are in keeping with the results of the present investigation apart from the absence of cardiac denervation found in PSP. The absence of an abnormality in PSP reported by Orimo et al. (41) may be attributable to the small sample of patients with PSP examined in their study ( $n = 5$ ).

No correlation was found between cardiac  $^{11}\text{C}$ -HED retention and striatal  $^{11}\text{C}$ -DTBZ binding. The patients with IPD, MSA, and PSP and with diminished cardiac retention also showed markedly decreased striatal presynaptic monoaminergic innervation, but several other patients with IPD, MSA, and PSP but without cardiac denervation showed striatal denervation. Four patients with MSA had normal or slightly decreased striatal innervation, and these patients showed principally ataxia with autonomic failure and relatively few features of parkinsonism. The lack of correlation between cardiac  $^{11}\text{C}$ -HED retention and striatal  $^{11}\text{C}$ -DTBZ binding suggests that the degenerative processes affecting the substantia nigra and the postganglionic cardiac sympathetic neurons occur independently. However, in contrast to our findings, a recent study of early IPD that assessed cardiac innervation with  $^{123}\text{I}$ -MIBG and striatal dopaminergic neurons with the dopamine reuptake inhibitor  $^{123}\text{I}$ - $N$ - $\omega$ -fluoropropyl-2 $\beta$ -carbomethoxy-3 $\beta$ -(4-iodophenyl)tropane ( $^{123}\text{I}$ -FP-CIT) did find a strong correlation between cardiac denervation and nigrostriatal denervation (42). In that study of 18 patients with early IPD, Spiegel et al. found that binding of  $^{123}\text{I}$ -FP-CIT in the more affected striatum was highly correlated with  $^{123}\text{I}$ -MIBG retention (H/M ratio) (42). Using our  $^{11}\text{C}$ -HED retention data for cardiac innervation and striatal  $^{11}\text{C}$ -DTBZ binding data for only the more affected striatum, we found no such relationship for our patients with IPD. One difference between our study and that of Spiegel et al. is that the latter investigators examined patients with early IPD (Hoehn–Yahr stage 1), whereas our patients with IPD had somewhat more advanced disease (Hoehn–Yahr stages 1.5–2.5). Some of their patients had normal or intermediate striatal binding of  $^{123}\text{I}$ -FP-CIT in the affected striatum, whereas all of our patients with IPD had substantial striatal denervation, as demonstrated by greatly reduced  $^{11}\text{C}$ -DTBZ binding. However, this difference in the stage of IPD between the 2 groups does not completely explain the difference in the findings. The data of Spiegel et al. suggest that if marked striatal denervation is observed in a patient with IPD when  $^{123}\text{I}$ -FP-CIT or  $^{11}\text{C}$ -DTBZ is used, then extensive cardiac denervation should also be found when either  $^{123}\text{I}$ -MIBG or  $^{11}\text{C}$ -HED is used. However, in the present study, we found that several patients with IPD (5/9) had greatly reduced striatal  $^{11}\text{C}$ -DTBZ binding but normal cardiac  $^{11}\text{C}$ -HED retention. In the cohort of patients with early IPD who were studied by Spiegel et al., no patients with this combination of normal heart innervation and substantial striatal denervation were seen. Thus, with the available data, we are unable to explain the apparent difference between our findings and those of Spiegel et al. A more focused study, ideally following the progression of striatal denervation and cardiac denervation in a large group of patients with early IPD, is likely needed to better characterize the relationship between these 2 processes.

The reductions in cardiac  $^{11}\text{C}$ -HED retention and striatal  $^{11}\text{C}$ -DTBZ binding observed in the present study are unlikely to have been caused by medication effects. It is well

established that  $^{11}\text{C}$ -HED is taken up into cardiac sympathetic neurons exclusively by NET (23), which is not significantly affected by SSRIs, trazodone, or bupropion (34). Although we observed severe global decreases in  $^{11}\text{C}$ -HED uptake in some patients taking SSRIs and trazodone, we also observed completely normal uptake in other patients taking these same medications at comparable doses. Levodopa is a very low-affinity substrate for NET (43), but no correlation was found between its use and the presence of  $^{11}\text{C}$ -HED retention deficits. In  $^{11}\text{C}$ -DTBZ studies of VMAT2 density in the brain, although many of our patients were taking either levodopa (a dopamine precursor) or pramipexole (a dopamine receptor agonist), the neuronal processing of these medications is different from that of  $^{11}\text{C}$ -DTBZ. Experimental *in vivo* studies have demonstrated that levodopa and dopamine receptor agonists do not affect the uptake of VMAT2 radioligands such as  $^{11}\text{C}$ -DTBZ (44). Thus, it seems likely that the substantial deficits in  $^{11}\text{C}$ -HED uptake and  $^{11}\text{C}$ -DTBZ binding observed in several of our patients resulted from denervation and not from medication effects.

## CONCLUSION

PET with  $^{11}\text{C}$ -HED demonstrated that significant losses of myocardial sympathetic nerve fibers occur not only in patients with IPD but also in some patients with the parkinsonian syndromes MSA and PSP. In all patients with IPD and with reduced  $^{11}\text{C}$ -HED retention, sympathetic denervation consistently was found to occur throughout the entire left ventricle. Although some patients with MSA also had complete left ventricular denervation, some patients with MSA and PSP had only focal regions of denervation. In light of these findings, it appears that the scintigraphic detection of cardiac sympathetic denervation alone cannot be used to differentiate IPD from MSA and PSP. Cardiac denervation was found not to be correlated with striatal denervation, suggesting that the neurodegenerative processes in these tissues occur independently. These findings advance the understanding of the incidence and progression of cardiac denervation in parkinsonian syndromes.

## ACKNOWLEDGMENTS

We thank the staff of the University of Michigan Cyclotron/PET Facility for assistance in preparing the PET radiopharmaceuticals and performing the PET imaging studies. This work was supported by grants from the National Institutes of Health (National Institute of Neurological Disorders and Stroke grant P01 NS15655; National Institute on Aging grant P50 AG08671; and National Heart, Lung, and Blood Institute grant R01 HL079540).

## REFERENCES

1. Senard JM, Valet P, Durrieu G, et al. Adrenergic supersensitivity in parkinsonians with orthostatic hypotension. *Eur J Clin Invest*. 1990;20:613–619.
2. Hirayama M, Hakusui S, Koike Y, et al. A scintigraphical qualitative analysis of peripheral vascular sympathetic function with meta- $^{123}\text{I}$ iodobenzylguanidine

- in neurological patients with autonomic failure. *J Auton Nerv Syst.* 1995;53:230–234.
3. Satoh A, Serita T, Tsujihata M. Total defect of metaiodobenzylguanidine (MIBG) imaging on heart in Parkinson's disease: assessment of cardiac sympathetic denervation [in Japanese]. *Nippon Rinsho.* 1997;55:202–206.
  4. Yoshita M, Hayashi M, Hirai S. Iodine 123-labeled meta-iodobenzylguanidine myocardial scintigraphy in the cases of idiopathic Parkinson's disease, multiple system atrophy, and progressive supranuclear palsy [in Japanese]. *Rinsho Shinkeigaku.* 1997;37:476–482.
  5. Yoshita M, Hayashi M, Hirai S. Decreased myocardial accumulation of <sup>123</sup>I-meta-iodobenzyl guanidine in Parkinson's disease. *Nucl Med Commun.* 1998;19:137–142.
  6. Yoshita M. Differentiation of idiopathic Parkinson's disease from striatonigral degeneration and progressive supranuclear palsy using iodine-123 meta-iodobenzylguanidine myocardial scintigraphy. *J Neurol Sci.* 1998;155:60–67.
  7. Iwasa K, Nakajima K, Yoshikawa H, Tada A, Taki J, Takamori M. Decreased myocardial <sup>123</sup>I-MIBG uptake in Parkinson's disease. *Acta Neurol Scand.* 1998;97:303–306.
  8. Satoh A, Serita T, Seto M, et al. Loss of <sup>123</sup>I-MIBG uptake by the heart in Parkinson's disease: assessment of cardiac sympathetic denervation and diagnostic value. *J Nucl Med.* 1999;40:371–375.
  9. Braune S, Reinhardt M, Schnitzer R, Riedel A, Lucking CH. Cardiac uptake of [<sup>123</sup>I]MIBG separates Parkinson's disease from multiple system atrophy. *Neurology.* 1999;53:1020–1025.
  10. Orimo S, Ozawa E, Nakade S, Sugimoto T, Mizusawa H. (123)I-Metaiodobenzylguanidine myocardial scintigraphy in Parkinson's disease. *J Neurol Neurosurg Psychiatry.* 1999;67:189–194.
  11. Druschky A, Hilz MJ, Platsch G, et al. Differentiation of Parkinson's disease and multiple system atrophy in early disease stages by means of I-123-MIBG-SPECT. *J Neurol Sci.* 2000;175:3–12.
  12. Reinhardt MJ, Jungling FD, Krause TM, Braune S. Scintigraphic differentiation between two forms of primary dysautonomia early after onset of autonomic dysfunction: value of cardiac and pulmonary iodine-123 MIBG uptake. *Eur J Nucl Med.* 2000;27:595–600.
  13. Taki J, Nakajima K, Hwang EH, et al. Peripheral sympathetic dysfunction in patients with Parkinson's disease without autonomic failure is heart selective and disease specific. *Eur J Nucl Med.* 2000;27:566–573.
  14. Takatsu H, Nishida H, Matsuo H, et al. Cardiac sympathetic denervation from the early stage of Parkinson's disease: clinical and experimental studies with radiolabeled MIBG. *J Nucl Med.* 2000;41:71–77.
  15. Takatsu H, Nagashima K, Murase M, et al. Differentiating Parkinson disease from multiple-system atrophy by measuring cardiac iodine-123 metaiodobenzylguanidine accumulation. *JAMA.* 2000;284:44–45.
  16. Orimo S, Ozawa E, Oka T, et al. Different histopathology accounting for a decrease in myocardial MIBG uptake in PD and MSA. *Neurology.* 2001;57:1140–1141.
  17. Courbon F, Brefel-Courbon C, Thalamas C, et al. Cardiac MIBG scintigraphy is a sensitive tool for detecting cardiac sympathetic denervation in Parkinson's disease. *Mov Disord.* 2003;18:890–897.
  18. Taki J, Yoshita M, Yamada M, Tonami N. Significance of <sup>123</sup>I-MIBG scintigraphy as a pathophysiological indicator in the assessment of Parkinson's disease and related disorders: it can be a specific marker for Lewy body disease. *Ann Nucl Med.* 2004;18:453–461.
  19. Berding G, Schrader CH, Peschel T, et al. [N-methyl <sup>11</sup>C]meta-Hydroxyephedrine positron emission tomography in Parkinson's disease and multiple system atrophy. *Eur J Nucl Med Mol Imaging.* 2003;30:127–131.
  20. Wakabayashi K, Takahashi H. Neuropathology of autonomic nervous system in Parkinson's disease. *Eur Neurol.* 1997;38(suppl 2):2–7.
  21. Goldstein DS, Holmes CS, Li ST, Bruce S, Metman LV, Cannon RO. Cardiac sympathetic denervation in Parkinson disease. *Ann Intern Med.* 2000;133:338–347.
  22. Nagayama H, Hamamoto M, Ueda M, Nagashima J, Katayama Y. Reliability of MIBG myocardial scintigraphy in the diagnosis of Parkinson's disease. *J Neurol Neurosurg Psychiatry.* 2005;76:249–251.
  23. Raffel DM, Wieland DM. Assessment of cardiac sympathetic nerve integrity with positron emission tomography. *Nucl Med Biol.* 2001;28:541–559.
  24. Bengel FM, Schwaiger M. Assessment of cardiac sympathetic neuronal function using PET imaging. *J Nucl Cardiol.* 2004;11:603–616.
  25. Gilman S, Raffel DM, Koeppe RA, et al. Cardiac sympathetic innervation in multiple system atrophy and progressive supranuclear palsy [abstract]. *Mov Disord.* 2004;19:1126.
  26. Gelb DJ, Oliver E, Gilman S. Diagnostic criteria for Parkinson's disease. *Arch Neurol.* 1999;56:33–39.
  27. Gilman S, Low PA, Quinn N, et al. Consensus statement on the diagnosis of multiple system atrophy. *J Auton Nerv Syst.* 1998;74:189–192.
  28. Litvan I, Agid Y, Calne D, et al. Clinical research criteria for the diagnosis of progressive supranuclear palsy (Steele-Richardson-Olszewski syndrome): report of the NINDS-SPSP international workshop. *Neurology.* 1996;47:1–9.
  29. Allman KC, Stevens MJ, Wieland DM, Wolfe ER, Greene DA, Schwaiger M. Noninvasive assessment of cardiac diabetic neuropathy by C-11 hydroxyephedrine and positron emission tomography. *J Am Coll Cardiol.* 1993;22:1425–1432.
  30. Hattori N, Tamaki N, Hayashi T, et al. Regional abnormality of iodine-123-MIBG in diabetic hearts. *J Nucl Med.* 1996;37:1985–1990.
  31. Stevens MJ, Raffel DM, Allman KC, et al. Cardiac sympathetic dysinnervation in diabetes: implications for enhanced cardiovascular risk. *Circulation.* 1998;98:961–968.
  32. Melon PG, Boyd CJ, McVey S, Mangner TJ, Wieland DM, Schwaiger M. Effects of active chronic cocaine use on cardiac sympathetic neuronal function assessed by carbon-11-hydroxyephedrine. *J Nucl Med.* 1997;38:451–456.
  33. Malizia AL, Melichar JK, Rhodes CG, et al. Desipramine binding to noradrenaline reuptake sites in cardiac sympathetic neurons in man in vivo. *Eur J Pharmacol.* 2000;391:263–267.
  34. Tatsumi M, Groshan K, Blakely RD, Richelson E. Pharmacological profile of antidepressants and related compounds at human monoamine transporters. *Eur J Pharmacol.* 1997;340:249–258.
  35. Rosenspire KC, Haka MS, Van Dort ME, et al. Synthesis and preliminary evaluation of carbon-11-meta-hydroxyephedrine: a false transmitter agent for heart neuronal imaging. *J Nucl Med.* 1990;31:1328–1334.
  36. Jewett DM, Kilbourn MR, Lee LC. A simple synthesis of [<sup>11</sup>C]dihydrotetrabenazine (DTBZ). *Nucl Med Biol.* 1997;24:197–199.
  37. Logan J, Fowler JS, Volkow ND, Wang GJ, Ding YS, Alexoff DL. Distribution volume ratios without blood sampling from graphical analysis of PET data. *J Cereb Blood Flow Metab.* 1996;16:834–840.
  38. Raffel DM, Corbett JR, del Rosario RB, et al. Clinical evaluation of carbon-11-phenylephrine: MAO-sensitive marker of cardiac sympathetic neurons. *J Nucl Med.* 1996;37:1923–1931.
  39. Sone M, Yoshida M, Hashizume Y, Hishikawa N, Sobue G. Alpha-synuclein-immunoreactive structure formation is enhanced in sympathetic ganglia of patients with multiple system atrophy. *Acta Neuropathol (Berl).* 2005;110:19–26.
  40. Kikkawa Y, Asahina M, Suzuki A, Hattori T. Cutaneous sympathetic function and cardiovascular function in patients with progressive supranuclear palsy and Parkinson's disease. *Parkinsonism Relat Disord.* 2003;10:101–106.
  41. Orimo S, Amino T, Itoh Y, et al. Cardiac sympathetic denervation precedes neuronal loss in the sympathetic ganglia in Lewy body disease. *Acta Neuropathol (Berl).* 2005;109:583–588.
  42. Spiegel J, Möllers M-O, Jost WH, et al. FP-CIT and MIBG scintigraphy in early Parkinson's disease. *Mov Disord.* 2005;20:552–561.
  43. Burgen ASV, Iversen LL. The inhibition of noradrenaline uptake by sympathomimetic amines in the rat isolated heart. *Br J Pharmacol.* 1965;25:34–49.
  44. Vander Borgh T, Kilbourn M, Desmond T, Kuhl D, Frey K. The vesicular monoamine transporter is not regulated by dopaminergic drug treatments. *Eur J Pharmacol.* 1995;294:577–583.